Available online at www.sciencedirect.com

ScienceDirect

materialstoday: PROCEEDINGS

ICMPC-2020

An Investigation on the Top Burr Formation during Minimum Quantity Lubrication (MQL) Assisted Micromilling of Copper

Suman Saha[1], A. Sravan Kumar, Sankha Deb, Partha Pratim Bandyopadhyay

Department of Mechanical Engineering, Indian Institute of Technology Kharagpur, Kharagpur, West Bengal, India, PIN – 721302
[1]Corresponding author: ss.me.kgp@iitkgp.ac.in

Abstract

Micromilling is one subtractive manufacturing process where excess material is gradually removed from the workpiece in the form of micro-chips with the help of a miniaturized cutting tool in order to fabricate three-dimensional micro-features. Burr formation in micromilling is one important problem as excessive burr hampers dimensional accuracy and functional requirements of the miniaturized features. Top-burr formation in micromilling is attributed to the lateral plastic deformation of the workpiece material when a rounded edge of the tool compresses it. This article explores the role of spindle speed and axial depth of cut on top-burr formation during micromilling of industrially pure copper samples using 0.5 mm TiAlN coated tungsten carbide micro end mills in MQL cutting environment. It is observed that down milling side top-burrs are significantly wider and larger as compared to that of the up milling side. For constant spindle speed, the average top-burr width is found to increase with axial depth for both up and down milling sides. However, the average top-burr width decreases marginally with the increase in spindle speed. In both up and down milling sides, the influence of depth of cut on top-burr width is more pronounced as compared to the influence of spindle speed. It was also observed that the difference between down milling top-burr width and up milling top-burr width does not vary appreciably with spindle speed.

Keywords: Micro-milling; MQL; Top Burr; Burr Formation; Spindle Speed; Axial Depth of Cut

1. Introduction

Micromilling is one subtractive manufacturing process where excess material is gradually removed from the workpiece in the form of micro-chips with the help of a miniaturized cutting tool in order to fabricate three-dimensional micro-features. The process is capable in producing several miniaturized features including slots, channels, fins, webs, pillars, pockets, dimples, cavities, etc. [1] Tool diameter, which is commonly used as the parameter for differentiating the micro-milling from macro-milling, typically varies in the range of 0.01 – 1.0 mm. Although Aurich et al. (2012) [2] showed the feasibility of micromilling of Ti-6Al-4V alloy with 20 µm diameter tool and PMMA polymer with 10 µm diameter tool, tools with diameter below 100 µm are seldom used owing to very small tool life mostly imposed by lack of rigidity. The inherent benefits of productivity and ease of restrictions on workroom environment paved the way for rapid development of the micro-end milling process [3]. Although the process offers several benefits, its performance is sometimes limited by the inherent burr formation, residual stress development, inaccuracy caused by progressive tool wear, size-effect, etc.

In metal cutting, burr is a part of workpiece material that is deformed plastically owing to the force exerted by the cutting tool but fails to separate completely from the workpiece. Burrs remain firmly attached to the open edges of the machined feature even after the completion of machining. Similar to chip formation, burr formation is also inherent to every tool based machining process, including macro-scale processes (such as conventional turning,

facing, drilling, milling, shaping, planing, etc.) and micro-scale processes (such as micro-milling, diamond turning, micro-drilling, etc.). The shape, size and location of formation, however, vary from one process to another and also depend on process parameters and tool geometry. Although the burr formation cannot be eliminated completely, its formation during machining can be minimized either through proper control of parameters [4] or by employing additional strategy (like using supporting material) [5]. Generated burrs can also be removed by deburring operations. However, deburring processes always incur additional cost, effort and time, and are mostly associated with the risk of undesired damage to the actual feature [6]. Thus minimization of burr formation through process control is better solution to get rid of excessive burrs. Presence of excessive burrs on the machined components has several disadvantages, as enlisted below.

- Burr degrades appearance of the machined features
- It hampers dimensional accuracy of the components
- It also limits the functional requirements of the components
- It possess difficulty in assembly
- It also restricts smooth sliding motion on the surface
- Sometimes, it is associated with the injury risk during manual handling of the components

Lekkala et al. (2011) [7] investigated burr formation in low speed (up to 5000 rpm) micromilling and concluded that the cutter diameter, axial depth, number of tooth, and feed per flute have significant influence on burr formation. Liu et al. (2017) [8] studied cutting forces, burr formation, and wall deformation during fabricating thin wall structures of 600 μm height and 20, 45, 70 μm thickness on copper samples with varying spindle speeds (12000, 15000, 18000 rpm), feeds per flute (0.25, 0.50, 0.75 μm/flute), and radial immersions (10, 20, 30 μm). A 2-flute 0.5 mm diameter diamond coated micro-end mill having 6 μm edge radius was used for this purpose. It was observed that down milling mode produces less deformation and burr. Mian et al. (2011) [9] concluded that high cutting velocity helps reducing specific energy and improving surface finish. Kiswanto et al. (2014) [10] also investigated effects of spindle speed and feed rate on burr formation in micromilling of Aluminum AA 1100 alloy. It was observed that up milling produce smaller burrs as compared to down milling. Besides developing model of top-burr formation, Ray et al. (2019) [11] also concluded that top-burr width has an inverse relation with both feed per flute and spindle speed. However, top-burr width increases with axial depth of cut.

Machinability refers to the feasibility and ease of machining of a particular workpiece material with a specified cutting tool under given conditions. As mentioned by Bai et al. (2019), [12] lower cutting forces, less power consumption, low cutting temperature, less burr formation, favourable chips, improved surface integrity and extended tool life are the indications of good machinability. Application of proper cutting fluid during machining helps improving machinability. There are several fluid delivery technique, Minimum Quantity Lubrication (MQL) is one among them. In MQL technique, the cutting oil is directly delivered to the cutting zone in the form of tiny droplets after mixing with compressed air. A wide variety of oil flow rate is used in literature. In deep hole drilling, Heinemann et al. (2006) delivered oil at a flow rate of 18 ml/h [13]. During turning, Diniz et al. (2003) varied the oil flow rate from 10 – 60 ml/h [14] While slot milling on Ti-6Al-4V titanium alloy in MQL cutting environment using two-flute uncoated tungsten carbide end mills having 300 μm diameter, Mittal et al. (2018) [15] showed that the effects of lubrication may not be clearly observed during micromilling with speed lower than 40,000 rpm. Aslantas et al. (2018) [16] observed significantly lower top-burr width in MQL assisted micromilling at 20,000 rpm spindle speed as compared to the same in dry cutting. Objective of this investigation is to explore the role of spindle speed and axial depth of cut on top-burr formation during micromilling of industrially pure copper samples in MQL cutting environment. Top-burrs that form in up milling side and down milling side are reported separately.

2. Experimental details

Copper samples of 20 mm width, 20 mm length and 10 mm thickness are selected for current work. An island of 5 mm width and 3 mm height is first made at the middle of the sample by removing material from all sides. 0.5 mm width and 5 mm long straight slots are then cut by full immersion micromilling. The term full immersion in this context indicates that the width of the slot is theoretically equal to the diameter of micro end mill. Spindle speed and axial depth of cut are varied, as shown in Table-1. The feed rate, however, is maintained at 4 μm/flute to ensure material removal by every cutting edge in each revolution, as discussed in section-3. Entire machining operation is

carried out in MQL cutting environment on a Kern-Evo high precision micro-machining centre (KERN, Germany). UNILUBE 2032 (Unilube AG, Switzerland) cutting oil is delivered continuously into the cutting zone using two nozzles at a total flow rate of 6 mL/hr. The air pressure is maintained in between 6 – 8 bar.

Table-1: Process parameters for the current investigation

Feed per flute (µm/flute)	Spindle speed (rpm)	Axial depth of cut (µm)	Engagement angle	Cutting environment	Oil flow rate
2.0	15000, 25000, 35000, 45000	50, 100, 150, 200	180°	UNILUBE 2032 based MQL	6 mL/hr

Two-flute TiAlN coated tungsten carbide micro-end mills (Axis Microtools, India) of 500 µm diameter are used to cut micro-slots. The helix angle of the cutting tool is 30° and the edge radius (r_e) is 1.62 µm (Fig. 1). The cutting edges have a positive rake angle. Each slot is cut using a fresh tool. After machining, slots with top-burr are observed under a Scanning Electron Microscope (SEM) (EVO 18, ZEISS) in different magnifications. Such images are further analysed by AxioVision software to measure top-burr width.

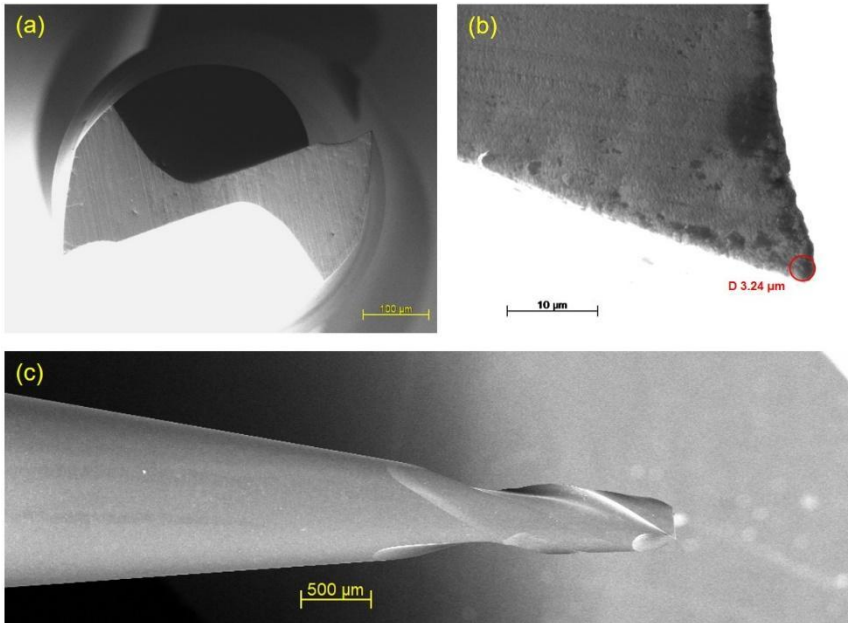

Fig. 1: SEM images of micro-end milling cutter (a) bottom view of the tool, (b) magnified view of the cutting edge indicating an edge radius of 1.62 µm, and (c) side view of the tool indicating helical cutting edge

3. Results and discussion

Since controlling the burr formation during machining is one fruitful action towards burr minimization, so it is essential to have knowledge on the influences of several factors including the tool geometry and process parameters on the burr formation. End milling process is inherently an intermittent cutting process as each cutting edge repeatedly engages and disengages with the workpiece in every revolution. In full immersion straight slot milling, ideally every tooth remains in physical contact with the workpiece material for 180° of one rotation, while it remains disengaged for the rest 180°. During the engagement period, the chip load (which is proportional to chip thickness) varies with the tool rotational angle, and thus up milling and down milling occur one after another in every rotation. As shown in Fig. 2, the chip thickness ahead of a cutting edge increases from zero to maximum in the up milling side. This chip thickness once again decreases from the maximum value to zero in down milling side. The maximum chip thickness for each cutting edge in each revolution is theoretically same with the feed per flute. Non-linear variation of the chip thickness with the angle of rotation of the cutting tool changes the material deformation

scenario throughout the engagement period.

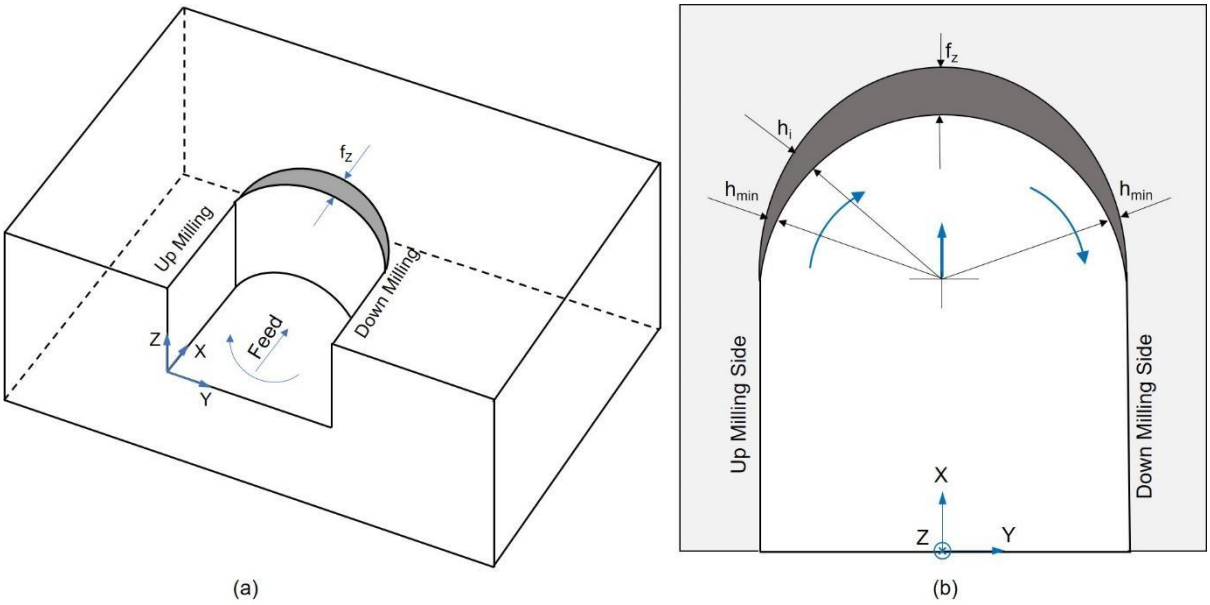

Fig. 2: Variation of chip thickness with the rotation of cutting edge during full immersion micromilling in (a) isometric view of the slot and (b) top view of the slot

Slender and overhanging micro-end milling tool cannot endure high feed per flute (f_Z). The f_Z value is typically maintained within the range of 0.05 – 6.0 µm/flute. This, when coupled with very high rotational speed of the spindle, fetches substantial feed rate in mm/min to maintain machining time reasonably low. But the comparable values of feed per flute and edge radius of the cutting tool imposes a limit on the shearing action as machining takes place at highly negative rake angle of the tool. Smooth shearing or chip formation takes place only when the uncut chip thickness exceeds certain value, called minimum uncut chip thickness (h_{min}). When this critical value is not achieved, the workpiece material either undergoes elastic deformation, or deforms plastically whenever the developed stress exceeds the yield strength of concerned workpiece material. Since the chip thickness in up milling side gradually increases from zero to maximum value (Fig. 2b), so the chip formation initiates only after certain angle of tool rotation from the beginning of engagement. The same phenomenon also happens in down milling side; however, in reverse order. In down milling side, tool-workpiece engagement initiates with maximum uncut chip thickness and gradually reaches to zero at the point of disengagement. Thus shearing prevails towards the beginning of down milling side; but once the uncut chip thickness drops below the h_{min} with the tool rotation, shearing transforms into plastic deformation and thus no further chip formation occurs.

It is worth mentioning in this context that if the given feed per flute value is lower than the minimum uncut chip thickness for a particular combination of workpiece-tool (i.e. $f_Z < h_{min}$), then chip formation is less likely to take place in every revolution by each cutting edge. Instead, both the elastic-plastic deformation of the workpiece material and also the deflection of the tool in a direction opposite to the feed simultaneously take place for a certain number of revolutions. As soon as the total thickness of accumulated workpiece material ahead of the tool reaches the intended h_{min}, entire material is removed in one pass. Alternatively, if the bending stress induced due to the deflection of tool exceeds the flexural strength limit, then catastrophic failure is also likely to happen. In this investigation, feed per flute is taken as 2 µm/flute, whereas the edge radius of the tool is $r_e = 1.62$ µm. The h_{min} value estimated by Rezaei et al. (2018) [17] in MQL cutting environment is 15 – 34% of the edge radius. The feed of 2 µm/flute selected in this investigation is adequately higher than the 34% of r_e value (i.e. 0.55 µm). This ensures chip formation in every rotation by each cutting edge. Furthermore, as the selected f_Z is higher than h_{min}, so elastic deformation, plastic deformation and shearing are expected to happen simultaneously in both up and down milling sides in every rotation by each cutting edge. While the elastic deformation is regained after the tool passes over it, the plastic deformation causes lateral flow of material in the form of top burr, and the shearing leads to chip formation.

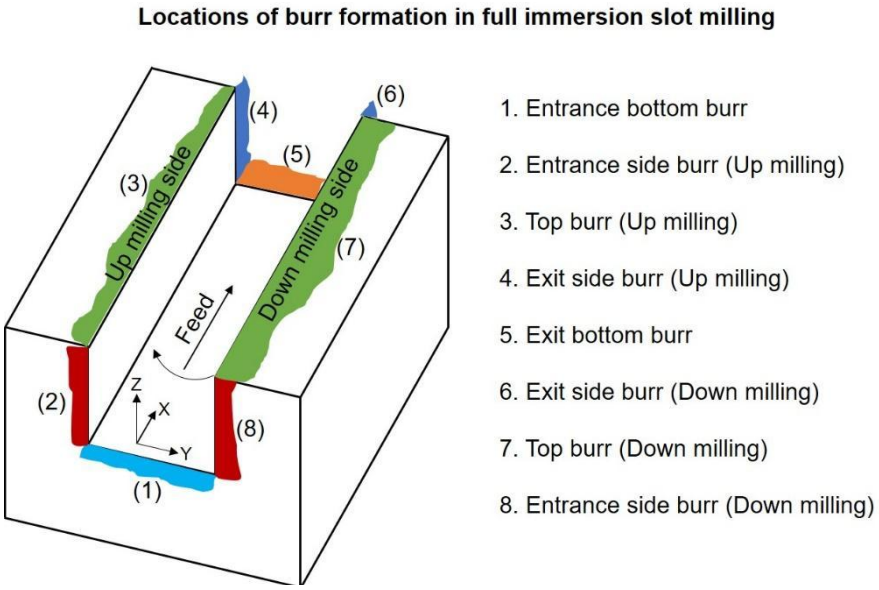

Fig. 3: Location of different burrs that form during full immersion micromilling of through slots

ISO 13715:2017 specifies standard rules for the indication and dimensioning of undefined edges (such as burrs, flash, etc.). Based on the mechanism of formation in macro-scale end-milling, Gillespie (1976) classified burrs into four different types, namely Poisson burr, roll-over burr, tear burr, and cut-off burr [18]. Based on the location of formation in full immersion straight slot milling, burrs can once again be divided into eight types, as shown in Fig. 3. Top-burrs are mainly Poisson burr. It forms owing to the lateral plastic deformation of the workpiece material when compressive force is exerted by a cylinder [19]. Since cutting edge radius (r_e) of the micro end mill is comparable to the feed per flute (f_z), so this rounded cutting edge within the axial depth of cut (a_p) acts as a cylinder. Accordingly, top burr formation in micro end milling occurs when this rounded cutting edge rotates following its own trajectory compressing the workpiece material.

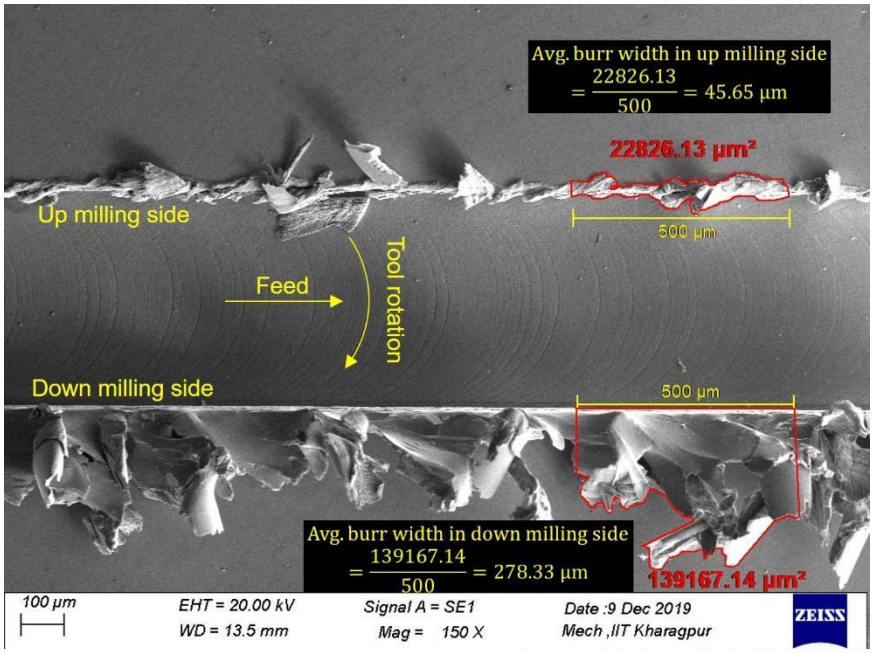

Fig. 4: Measurement of average top-burr width from the burr area (N = 25,000 rpm, a_p = 100 µm, f_z = 2 µm/flute)

Top-burrs usually have a non-uniform shape. Accordingly, its width (measured perpendicular to feed direction) varied from one point to another. Thus an average burr width based on the surface area is used here for analysis. This average burr width measurement is based on the principle of projecting irregular and non-uniform burrs into an equivalent rectangular shaped burr, where both have same surface area and length but different width. A similar method was reported by Medeossi et al. (2018) [20]. However, instead of using non-contact type profilometer, the average burr width is measured by analysing the SEM images. As machined slots are first observed under SEM. The actual profile of the burr on such SEM images is marked using the AxioVision software (Fig. 4). A sample length of 0.5 mm is considered here. The surface area of the top-burr within this sample length is measured. This area is then divided by the sample length to obtain an average top-burr width. Burrs in up milling side and down milling side are reported separately.

As shown in Fig. 4, top-burr formation occurs in both up and down milling sides; however, burrs in down milling side is significantly larger as compared to the up milling side. In full immersion slot milling, up milling is preceded by down milling. Once the chip formation starts in up milling side, it continues for the rest of the tool rotation. Thus whenever the instantaneous uncut chip thickness exceeds the intended h_{min} value, chip formation starts. Accordingly, one layer of chip (say i^{th} layer) that formed earlier is pushed by the next layer of chip (say $i+1^{th}$ layer). This assists in complete chip separation as the uncut chip thickness for $i+1^{th}$ layer is higher than that of i^{th} layer. However, in the down milling side, uncut chip thickness gradually decreases with tool rotation. Accordingly, the force exerted by the i^{th} layer on the $i+1^{th}$ layer is less. Accordingly, the chips lose momentum to flow continuously, especially towards the end of down milling side [19]. Some of these chips fail to separate completely from the workpiece and remain attached to the edges in the form of burr. Hence, top-burr on the down milling side becomes significantly higher than that for up milling side.

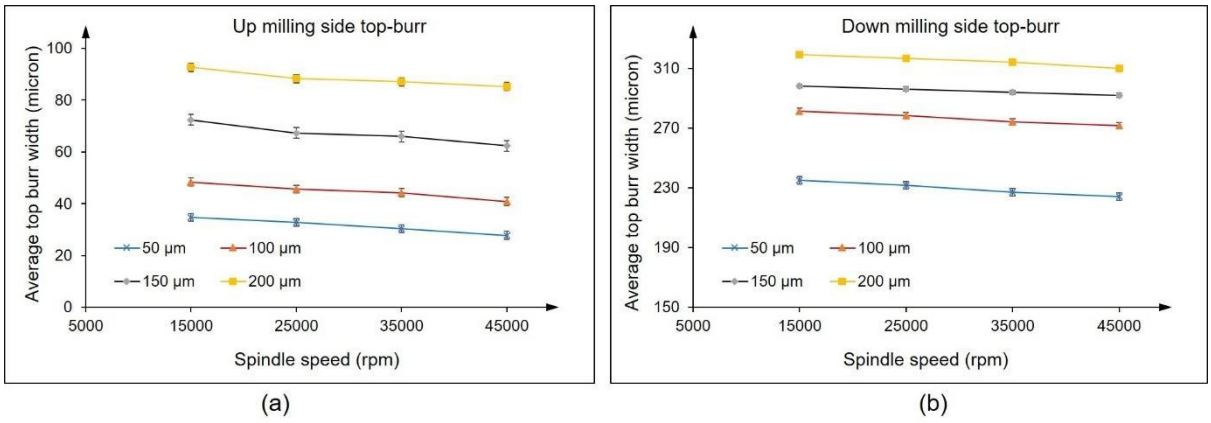

Fig. 5: Variation of average top-burr width with spindle speed and axial depth for (a) up milling side and (b) down milling side

Variation of average up milling top-burr width with spindle speed for different axial depths is shown in Fig. 5. Since the volume of the workpiece material that is undergoing plastic deformation increases proportionally with the axial depth of cut, so top-burr width is also expected to increase with axial depth. The same can be observed in Fig. 5a. However, for a constant axial depth, top-burr width decreases with increase in spindle speed. Similar to up-milling side, the down milling top-burr width also has a proportional relationship with axial depth of cut (Fig. 5b). The decreasing trend of top-burr width with increase in spindle speed is also observed in down milling. Moreover, a steep change on top-burr width can be noticed with the alteration in axial depth, whereas, such change is small for the variation in spindle speed. This is true in both up and down milling sides. Thus it can be inferred that the influence of depth of cut on top-burr width is more pronounced as compared to the influence of spindle speed.

Since the down milling side generates wider burr as compared to the same for up milling side, so the difference in top burr width between down milling and up milling is plotted against spindle speed for varying axial depth (Fig. 6). It is interesting to observe that the difference does not vary appreciably with spindle speed. This is true for every depth of cut investigated here. It indicates that the influence of spindle speed is more or less same for both up and down milling sides.

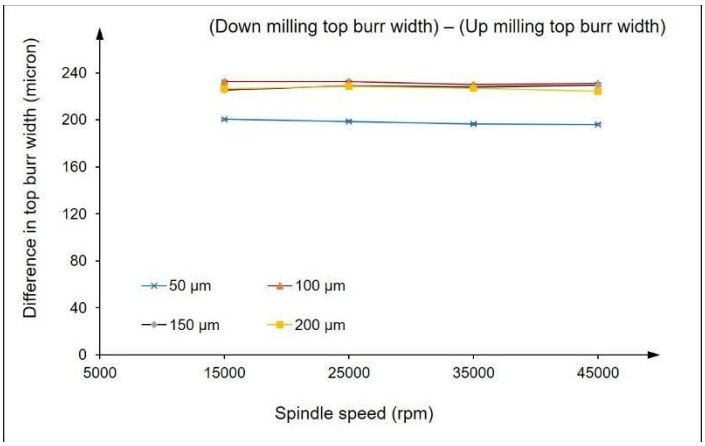

Fig. 6: Variation of the difference between down milling top-burr width and up milling top-burr width with spindle speed and axial depth

Conclusions

1. Down milling generates significantly wider and larger top-burrs as compared to up milling side. This is possibly owing to the lack of momentum for continuous flow of chips towards the end of down milling. Thus some of the chips at the end of down milling don't separate completely, rather remain attached with the workpiece in the form of burr.

2. For constant spindle speed, the average top-burr width increases with increase in axial depth for both up and down milling sides. This is owing to the fact that the volume of the workpiece material that is undergoing plastic deformation increases proportionally with the axial depth of cut. Since top-burr forms owing to lateral plastic deformation of workpiece material, so larger top-burr is obtained at higher axial depth.

3. Top-burr width, in both up and down milling sides, also drops marginally with the increase in spindle speed. However, the influence of depth of cut on top-burr width is more pronounced as compared to the influence of spindle speed. Thus axial depth is the most significant factor in terms of top-burr width.

4. The difference between down milling top-burr width and up milling top-burr width does not vary appreciably with spindle speed. Thus the influence of spindle speed on top-burr width is more or less same for both up and down milling sides.

Funding: This research did not receive any specific grant from funding agencies in the public, commercial, or not-for-profit sectors.

Declaration of interest: The authors don't have any conflict of interest to disclose.

References

[1] S. Zhang, Y. Zhou, H. Zhang, Z. Xiong, S. To, Advances in ultra-precision machining of micro-structured functional surfaces and their typical applications, International Journal of Machine Tools and Manufacture. 142 (2019) 16–41. https://doi.org/10.1016/j.ijmachtools.2019.04.009

[2] J.C. Aurich, I.G. Reichenbach, G.M. Schüler, Manufacture and application of ultra-small micro end mills, CIRP Annals. 61 (2012) 83–86. https://doi.org/10.1016/j.cirp.2012.03.012

[3] P.-C. Chen, C.-W. Pan, W.-C. Lee, K.-M. Li, An experimental study of micromilling parameters to manufacture microchannels on a PMMA substrate, The International Journal of Advanced Manufacturing Technology. 71 (2014) 1623–1630. https://doi.org/10.1007/s00170-013-5555-z

[4] S.A. Niknam, B. Davoodi, J.P. Davim, V. Songmene, Mechanical deburring and edge-finishing processes for aluminum parts—a review, The International Journal of Advanced Manufacturing Technology. 95 (2017) 1101–1125. https://doi.org/10.1007/s00170-017-1288-8
[5] Z. Kou, Y. Wan, Y. Cai, X. Liang, Z. Liu, Burr Controlling in Micro Milling with Supporting Material Method, Procedia Manufacturing. 1 (2015) 501–511. https://doi.org/10.1016/j.promfg.2015.09.015
[6] G. Mathai, S. Melkote, Effect of process parameters on the rate of abrasive assisted brush deburring of microgrooves, International Journal of Machine Tools and Manufacture. 57 (2012) 46–54. https://doi.org/10.1016/j.ijmachtools.2012.02.007
[7] R. Lekkala, V. Bajpai, R.K. Singh, S.S. Joshi, Characterization and modeling of burr formation in micro-end milling, Precision Engineering. 35 (2011) 625–637. https://doi.org/10.1016/j.precisioneng.2011.04.007
[8] Y. Liu, P. Li, K. Liu, Y. Zhang, Micro milling of copper thin wall structure, The International Journal of Advanced Manufacturing Technology. 90 (2016) 405–412. https://doi.org/10.1007/s00170-016-9334-5
[9] A. Mian, N. Driver, P. Mativenga, Identification of factors that dominate size effect in micro-machining, International Journal of Machine Tools and Manufacture. 51 (2011) 383–394. https://doi.org/10.1016/j.ijmachtools.2011.01.004
[10] G. Kiswanto, D. Zariatin, T. Ko, The effect of spindle speed, feed-rate and machining time to the surface roughness and burr formation of Aluminum Alloy 1100 in micro-milling operation, Journal of Manufacturing Processes. 16 (2014) 435–450. https://doi.org/10.1016/j.jmapro.2014.05.003
[11] D. Ray, A.B. Puri, N. Hanumaiah, S. Halder, Modeling of Top Burr Formation in Micro-End Milling of Zr-Based Bulk Metallic Glass, Journal of Micro and Nano-Manufacturing. 7 (2019). https://doi.org/10.1115/1.4045093
[12] W. Bai, A. Roy, R. Sun, V.V. Silberschmidt, Enhanced machinability of SiC-reinforced metal-matrix composite with hybrid turning, Journal of Materials Processing Technology. 268 (2019) 149–161. https://doi.org/10.1016/j.jmatprotec.2019.01.017
[13] R. Heinemann, S. Hinduja, G. Barrow, G. Petuelli, Effect of MQL on the tool life of small twist drills in deep-hole drilling, International Journal of Machine Tools and Manufacture. 46 (2006) 1–6. https://doi.org/10.1016/j.ijmachtools.2005.04.003
[14] A. Diniz, J. Ferreira, F. Filho, Influence of refrigeration/lubrication condition on SAE 52100 hardened steel turning at several cutting speeds, International Journal of Machine Tools and Manufacture. 43 (2003) 317–326. https://doi.org/10.1016/S0890-6955(02)00186-4
[15] R.K. Mittal, S.S. Kulkarni, R. Singh, Characterization of lubrication sensitivity on dynamic stability in high-speed micromilling of Ti–6Al–4V via a novel numerical scheme, International Journal of Mechanical Sciences. 142-143 (2018) 51–65. https://doi.org/10.1016/j.ijmecsci.2018.04.038
[16] K. Aslantas, A. Çiçek, The effects of cooling/lubrication techniques on cutting performance in micro-milling of Inconel 718 superalloy, Procedia CIRP. 77 (2018) 70–73. https://doi.org/10.1016/j.procir.2018.08.219
[17] H. Rezaei, M.H. Sadeghi, E. Budak, Determination of minimum uncut chip thickness under various machining conditions during micro-milling of Ti-6Al-4V, The International Journal of Advanced Manufacturing Technology. 95 (2017) 1617–1634. https://doi.org/10.1007/s00170-017-1329-3
[18] Gillespie, L. (1976). Burrs produced by end milling. https://doi.org/10.2172/7259917
[19] X. Wu, L. Li, N. He, Investigation on the burr formation mechanism in micro cutting, Precision Engineering. 47 (2017) 191–196. https://doi.org/10.1016/j.precisioneng.2016.08.004
[20] F. Medeossi, M. Sorgato, S. Bruschi, E. Savio, Novel method for burrs quantitative evaluation in micro-milling, Precision Engineering. 54 (2018) 379–387. https://doi.org/10.1016/j.precisioneng.2018.07.007

*Declaration of Interest Statement

Declaration of interests

☒ The authors declare that they have no known competing financial interests or personal relationships that could have appeared to influence the work reported in this paper.

☐The authors declare the following financial interests/personal relationships which may be considered as potential competing interests:

Figure-1

Click here to download high resolution image

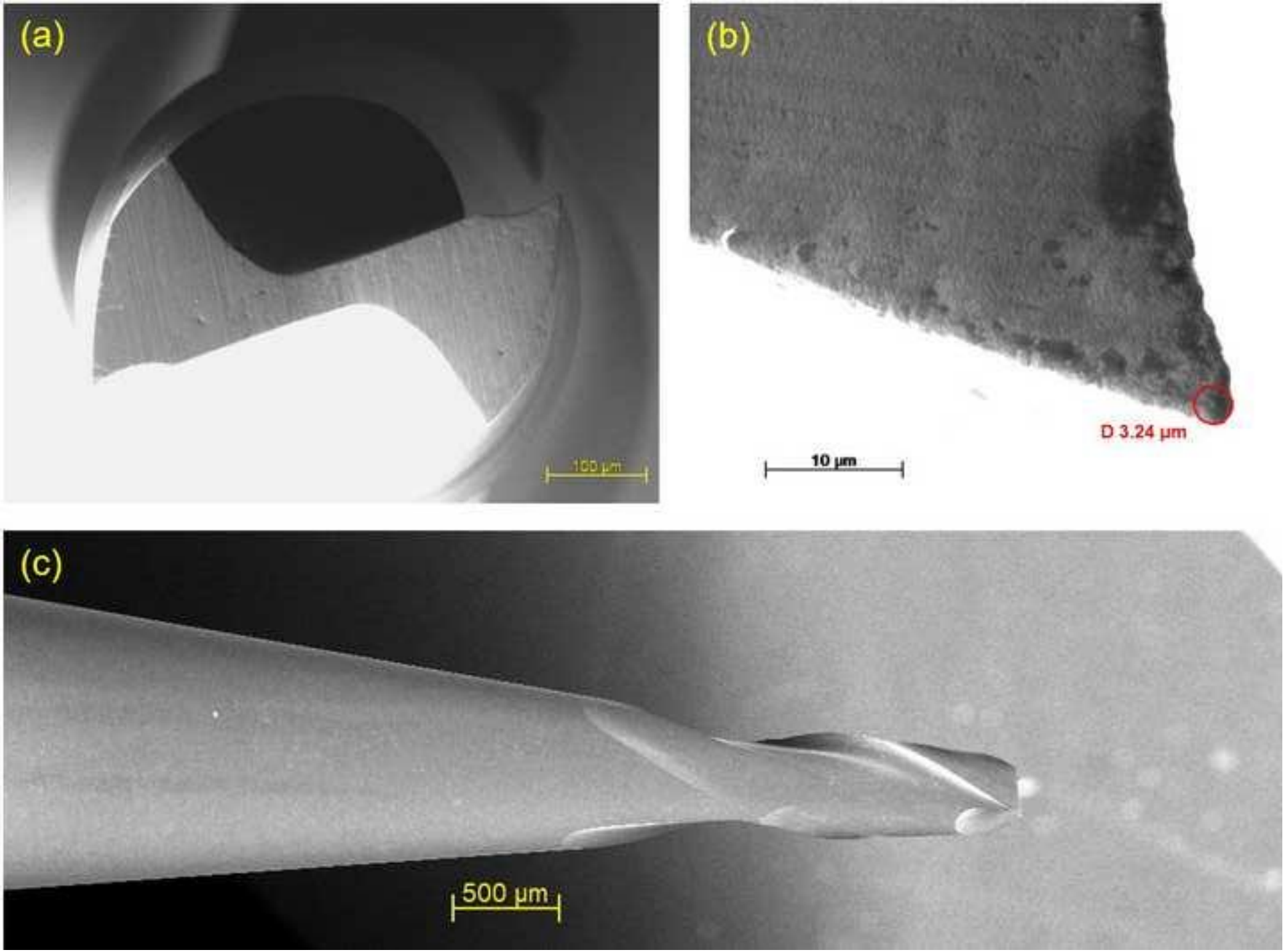

Figure-2
Click here to download high resolution image

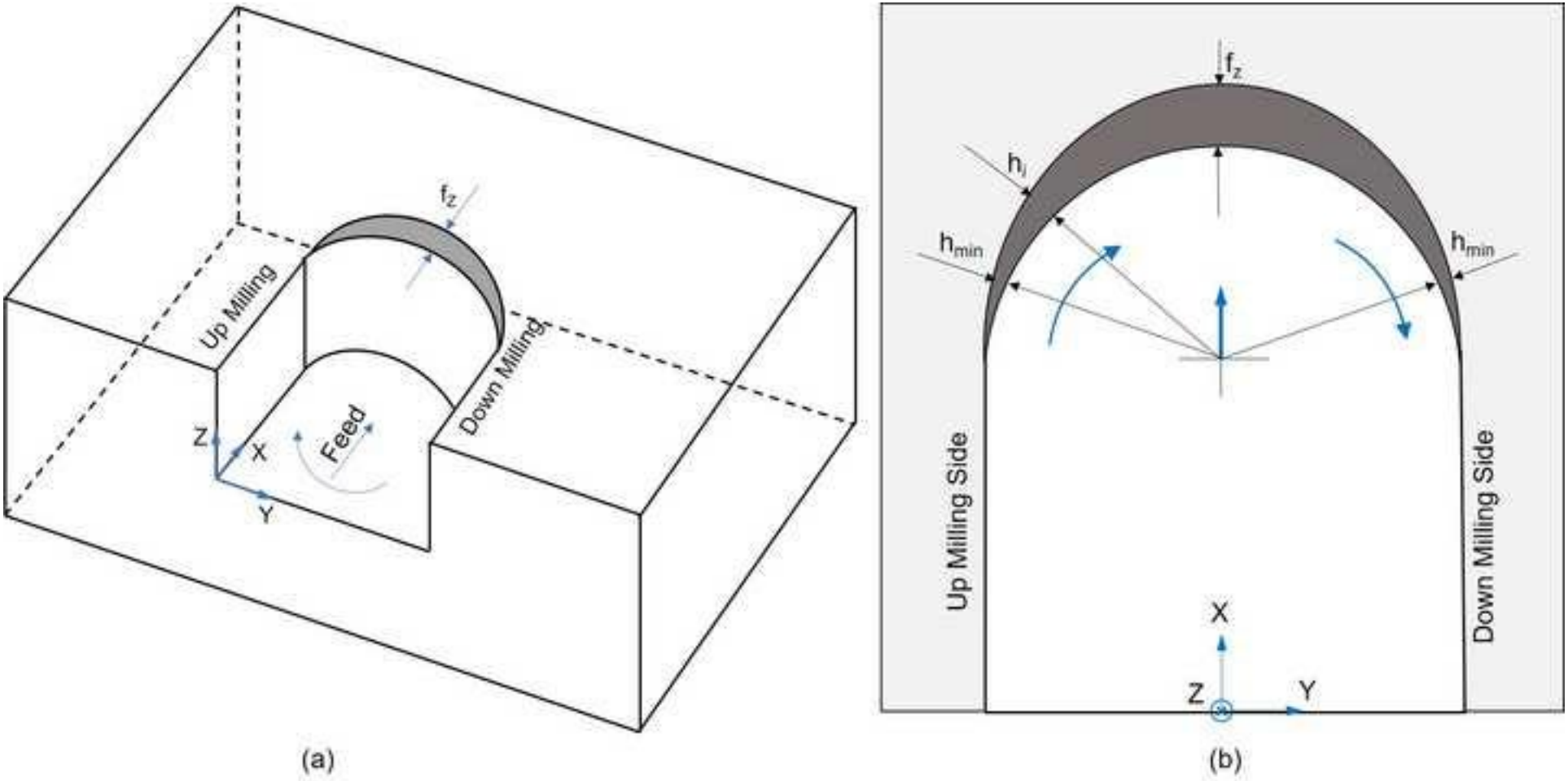

Figure-3
Click here to download high resolution image

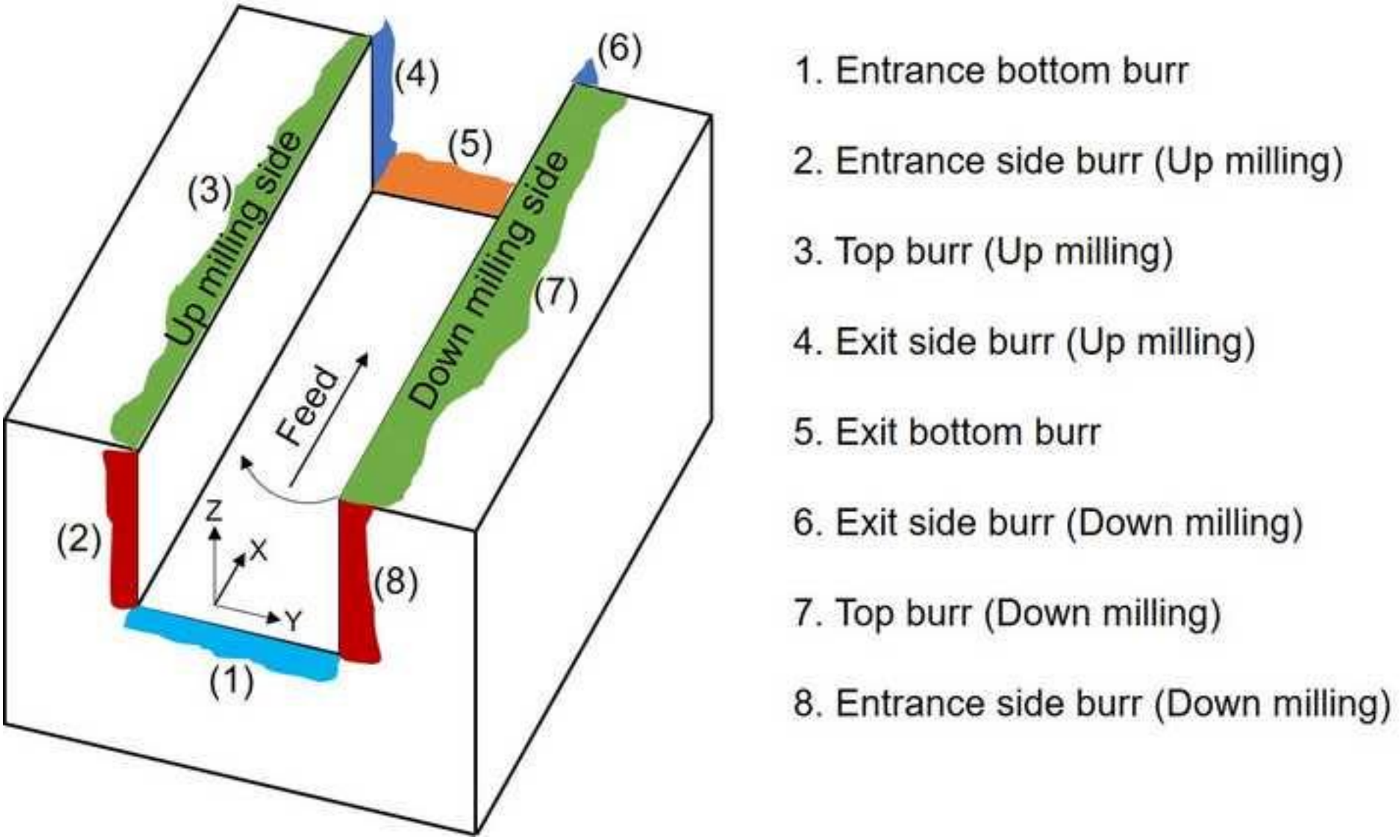

Figure-4

Click here to download high resolution image

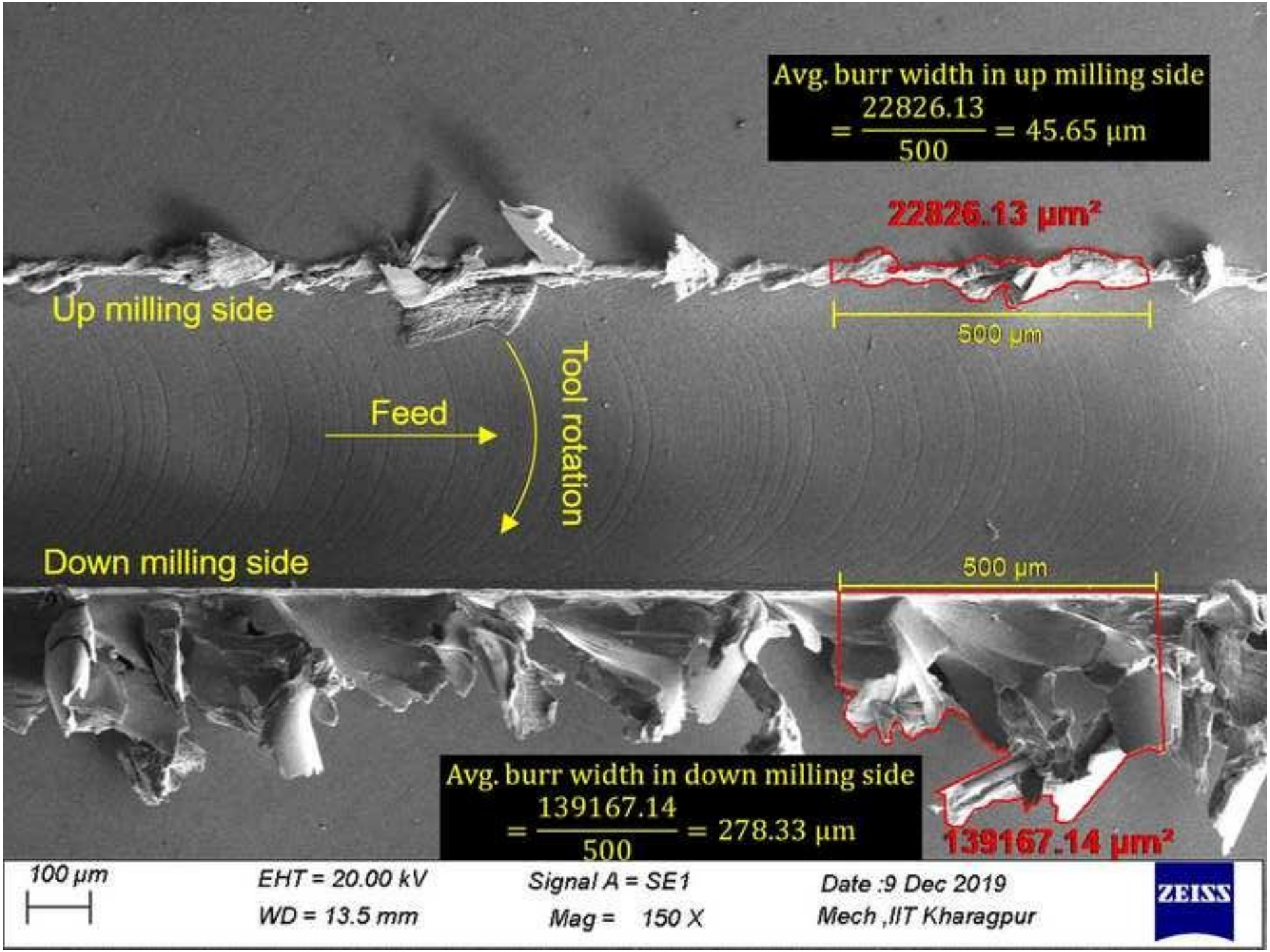

Figure-5
Click here to download high resolution image

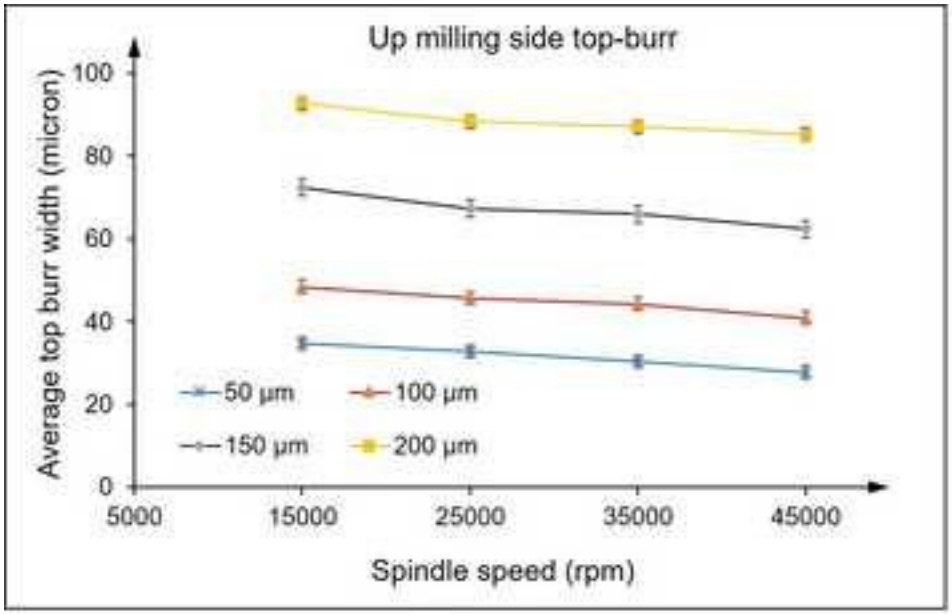

(a)

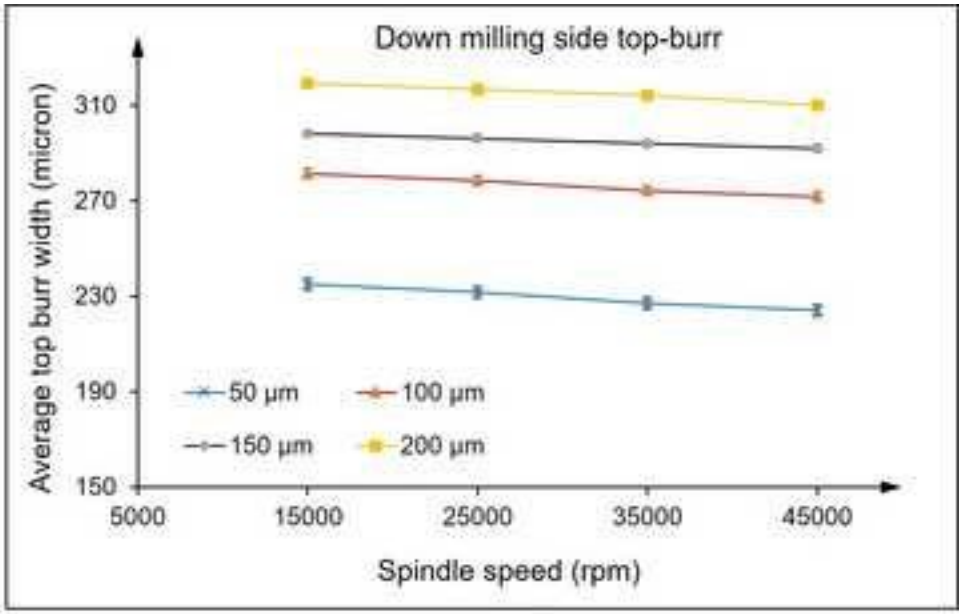

(b)

Figure-6

Click here to download high resolution image